

## Notes

Coil–Coil Interactions for Poly(dimethylsiloxane) in Compressible Supercritical CO<sub>2</sub>A. F. Kostko,<sup>†</sup> M. A. McHugh,<sup>\*,†</sup> and J. H. van Zanten<sup>\*,‡</sup>

Department of Chemical and Life Science Engineering,  
Virginia Commonwealth University,  
Richmond, Virginia 23284, and Department of Chemical and  
Biomolecular Engineering, North Carolina State University,  
Raleigh, North Carolina 27695-7905

Received October 27, 2005

Revised Manuscript Received December 16, 2005

Investigations of the solvent quality of a supercritical fluid solvent (SCF), such as CO<sub>2</sub>, has attracted academic and industrial interest for processing polymers.<sup>1,2</sup> Reliable applications of supercritical CO<sub>2</sub> technology require information on polymer–CO<sub>2</sub> phase behavior and on the solvent quality of CO<sub>2</sub> as a function of pressure or density. One measure of solvent quality is the second osmotic virial coefficient,  $A_2$ , which also provides information on the behavior of isolated polymer chains in solution.<sup>3,4</sup> As the solvent density is adjusted,  $A_2$  is anticipated to change from negative values at low densities and poor solvent quality where polymer chains contract slightly relative to their unperturbed size to positive values at high densities and good solvent quality where polymer chains expand relative to their unperturbed size. At the theta condition, where  $A_2$  is zero, repulsive excluded-volume interactions compensate attractive monomer–monomer interactions, and the polymer adapts its unperturbed size.

While  $A_2$  is typically determined by osmotic pressure or static light scattering (SLS) methods, both techniques are problematic to implement in a high-pressure environment with a highly compressible solvent. Our research group has utilized dynamic light scattering (DLS) to probe coil–coil interactions<sup>5,6</sup> since it is easier to identify and resolve potential artifacts associated with high-pressure scattering cells.<sup>6,7</sup> Coil–coil interactions are ascertained via the concentration,  $c$ , dependence of the polymer translational diffusion coefficient,  $D$ <sup>8</sup>

$$D = D_0[1 + k_D c + \dots] \quad (1)$$

where  $D_0$  is the infinite dilution diffusion coefficient and  $k_D$  is the dynamic second virial coefficient. Both thermodynamic and hydrodynamic (i.e., frictional) interactions are accounted for in  $k_D$ .<sup>9,10</sup>

$$k_D = 2A_2M - k_s + \frac{RT\kappa_T}{M} \quad (2)$$

where  $M$  is the polymer molar mass,  $k_s$  is the friction coefficient associated with the collective sedimentation coefficient,<sup>10</sup>  $R$  is

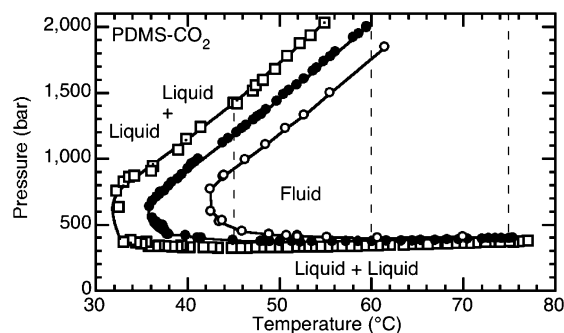


**Figure 1.** Phase behavior of 0.077 wt % (squares), 1.01 wt % (solid circles), and 7.0 wt % (open circles) PDMS in supercritical CO<sub>2</sub>. Lines through the data are to guide the eye, and the vertical dashed lines show the isothermal paths used for DLS measurements. The data have an accumulated error and reproducibility of  $\pm 15$  bar and  $\pm 0.2$  °C, except where the cloud-point curve changes slope, and it is more difficult to distinguish the phase-transition pressure.

the gas constant,  $T$  is the absolute temperature, and  $\kappa_T$  is the solution isothermal compressibility.<sup>9</sup> The third term is  $\sim O(10^{-6})$  and is neglected relative to the other terms.<sup>5</sup>

Cotts and Selser performed a particularly illustrative exposition of coil–coil interactions utilizing SLS and DLS with polymer covering a wide range of molecular weights.<sup>11</sup> To compare their study with related DLS investigations, it is more convenient to consider the polymer volume fraction,  $\phi$ , dependence of  $D$  to account for the effect of polymer molar mass

$$D = D_0[1 + k_D^\phi \phi + \dots] \quad (3a)$$

where

$$k_D^\phi = k_D \frac{M}{N_A V_H} \quad (3b)$$

Here,  $N_A$  is Avogadro's number and  $V_H$  is an equivalent hydrodynamic hard-sphere volume calculated with experimental values of the hydrodynamic radius  $R_H$ . Cotts and Selser<sup>11</sup> report the best estimate of the theta condition is  $k_D^\phi = -2$ , and the limit for good solvent conditions is  $k_D^\phi \cong 2$ .

Recently, Andre and co-workers investigated coil–coil interactions for poly(dimethylsiloxane) (PDMS)–CO<sub>2</sub> solutions<sup>12</sup> where they report that  $A_2$ , and the corresponding solvent quality, increase and appear to reach a maximum as the pressure is increased just near the pressure limit of their experimental apparatus. They were unable to probe the single-phase region shown in Figure 1 near the high-pressure, upper critical solution temperature (UCST) boundary of the PDMS–CO<sub>2</sub> system measured by the present authors. To the authors' best knowledge, this is the first time the high-pressure branch of the UCST has been reported for this system although Xiang and Kiran<sup>13</sup> reported on the low-pressure UCST branch up to  $\sim 620$  bar as well as the lower critical solution temperature boundary and the minimum in the boundary. The PDMS–CO<sub>2</sub> phase behavior

<sup>†</sup> Virginia Commonwealth University.

<sup>‡</sup> North Carolina State University.

\* Corresponding authors. E-mail: mmchugh@vcu.edu; john\_vz@ncsu.edu.

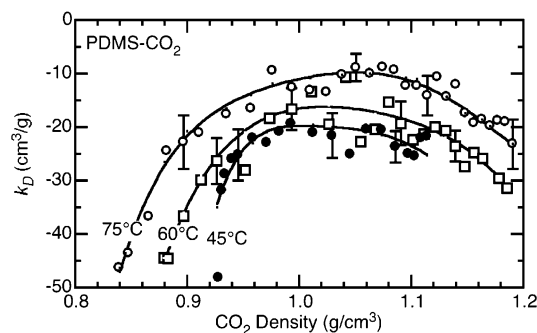


**Figure 2.** Dependence of the dynamic second virial coefficient on  $\text{CO}_2$  mass density at 45 °C (solid circles), 60 °C (squares), and 75 °C (open circles). The representative error bars shown here are the error associated with the fit of the data to eq 2.

is similar to that of the poly(ethylene-*co*-1-butene) (PEB<sub>10</sub>)–dimethyl ether (DME) system previously reported by the present authors.<sup>6</sup> Interestingly, DLS measurements for the PEB<sub>10</sub>–DME system revealed that solvent quality continually increases as the pressure is increased, starting at the low-pressure phase boundary and ending at the high-pressure UCST boundary, in contrast with the apparent maximum in solvent quality reported by Andre and co-workers<sup>12</sup> for the PDMS– $\text{CO}_2$  system. In this Note the existence of maximal solvent quality at intermediate pressures (densities) in the PDMS– $\text{CO}_2$  system is unequivocally demonstrated with DLS measurements over a wide pressure ( $\text{CO}_2$  density) range at 45, 60, and 75 °C near both high- and low-pressure phase boundaries shown in Figure 1.

PDMS ( $M_w = 75\,800$ ,  $M_w/M_n = 1.11$ ) is obtained from Polymer Source, Inc., and  $\text{CO}_2$  (99.999%) is obtained from BOC Gases. Details are given elsewhere<sup>5,6</sup> on the high-pressure scattering cell, DLS apparatus, and method of data analysis taking into account any pressure-induced changes in polymer concentration, solution viscosity, and solution refractive index. Teflon O-rings are used to seal the windows, and a spring-energized Teflon O-ring is used to seal the piston to avoid introducing contaminants that  $\text{CO}_2$  can leach from hydrocarbon O-rings. Also, pure  $\text{CO}_2$  rather than water is used as the pressurizing fluid to move the floating piston again to avoid introducing a contaminant into the polymer solution. The milklike scattering pattern of the laser beam at 90°, rather than the pattern from a conventional light source, provides a precise determination of the cloud point.  $D$  is obtained from autocorrelation functions via the cumulant method, and  $D_0$  and  $k_D$  are obtained from a linear, least-squares analysis of  $D$  as a function of concentration. The Supporting Information Section provides details on the determination of  $k_D$  from  $D$  vs  $c$  plots.  $R_H$  is obtained via the Stokes–Einstein relation,  $D_0 = kT/(6\pi\eta R_H)$ , where  $k$  is Boltzmann's constant and  $\eta$  is the viscosity of  $\text{CO}_2$ .<sup>14</sup>

Figure 2 shows experimentally determined  $k_D$  values as a function of  $\text{CO}_2$  density at 45, 60, and 75 °C. The existence of a fairly broad maximum in  $k_D$  at densities intermediate to those at the phase boundaries is readily apparent in contrast to the  $k_D$  values reported by Andre and co-workers.<sup>12</sup> There are two significant differences between the present study and that of Andre and co-workers. First, the present study explores a much larger  $\text{CO}_2$  density range, 0.84–1.19  $\text{g}/\text{cm}^3$  vs 0.97–1.04  $\text{g}/\text{cm}^3$ . This large density range is used at all temperatures in the present study to better elucidate the behavior of  $k_D$ . Second, a higher molar mass PDMS is used in the present study which accounts for the larger values of  $k_D$  observed here. The maximum in  $k_D$  observed in the present study demonstrates unequivocally the existence of maximal  $\text{CO}_2$  solvent quality for the PDMS– $\text{CO}_2$

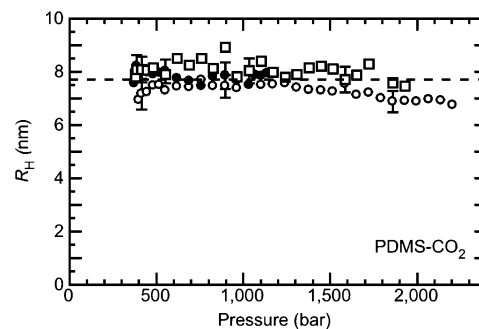


**Figure 3.** Dependence of the PDMS hydrodynamic radius on pressure at 45 °C (solid circles), 60 °C (squares), and 75 °C (open circles). The dashed line represents  $R_H$  averaged for all three temperatures. The representative error bars account for the error in  $D_0$  and in the viscosity of pure  $\text{CO}_2$ .

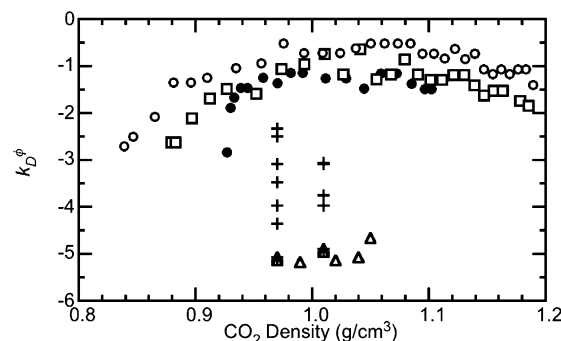


**Figure 4.** Dependence of the volume fraction-based, dynamic second virial coefficient,  $k_D^\phi$ , on  $\text{CO}_2$  density at 45 °C (solid circles), 60 °C (squares), and 75 °C (open circles) obtained in this study.  $k_D^\phi$  measurements of Andre and co-workers for a 31.3K molar mass PDMS are shown for 25 °C (triangles) and temperatures ranging from 30 to 54 °C for a density of 0.97  $\text{g}/\text{cm}^3$  and 30 to 42 °C for a density of 1.01  $\text{g}/\text{cm}^3$  (crosses).

system at intermediate densities in close agreement to the “apparent” maximum of  $A_2$  reported by Andre and co-workers.

Figure 3 shows that  $R_H$  is invariant with pressure (density). Although it may be argued that there is a weak maximum in  $R_H$  at intermediate pressures at 75 °C, this observation might simply be due to the precision of the experimental measurement (i.e., the polymer chains are not large enough to determine relative size changes). However, it is also plausible that slight changes in coil conformation may be offset by slight changes in coil draining characteristics. The invariant behavior of  $R_H$  of PDMS in  $\text{CO}_2$  is in agreement with that observed by Andre and co-workers. Our research group has observed essentially the same behavior for the PEB<sub>10</sub>–DME system where  $R_H$  was independent of temperature or DME density even though a higher molar mass polymer was considered.<sup>6</sup>

As noted previously, it is more convenient to consider the polymer volume fraction dependence of  $D$  as a means of accounting for the effect of polymer molar mass when comparing measurements made on different polymer samples. In Figure 4,  $k_D^\phi$  values as a function of  $\text{CO}_2$  density obtained in the present study are compared with those estimated from the data of Andre and co-workers<sup>12</sup> for a 31.3K molar mass PDMS. The greatly enhanced density range and easily discerned  $k_D^\phi$  maximum associated with the current study are immediately apparent. While the lower  $k_D^\phi$  values of Andre and co-workers are primarily a result of lower molar mass polymers and temperatures, the potential role of end effects being more prevalent in their samples cannot be entirely discounted. Also, the larger

molar mass PDMS investigated here provides greater sensitivity for the measured concentration dependence of  $D$  that is particularly important when the concentration dependence is weak.

The concentration dependence of  $D$  provides access to the second osmotic virial coefficient,  $A_2$ , since both the thermodynamic and hydrodynamic interactions are functions of  $A_2/R_H^3$ .<sup>11</sup> Therefore, the observed maximum in  $k_D^\phi$  corresponds to a maximum in  $A_2$ . On the basis of a previous observation of  $k_D^\phi = -2$  at the theta condition,<sup>11</sup> it is apparent that the low-pressure phase boundary occurs at sub-theta conditions since the measured  $k_D^\phi < -2$  at this low-density phase boundary. The  $k_D^\phi$  values estimated from the data of Andre and co-workers indicate sub-theta conditions in accordance with their measured negative  $A_2$  values.<sup>12</sup> Earlier high-pressure DLS studies with compressible solvents indicate that phase separation also occurs at sub-theta solvent quality for PEB<sub>10</sub>—simple alkane solutions,<sup>5</sup> while phase separation occurs *before* the onset of theta-solvent quality in the case of PEB<sub>10</sub>—DME solutions<sup>6</sup> at the low-pressure phase boundary. It is likely that the low-pressure phase boundary results from a solvent whose density is not sufficient to effectively screen intramolecular monomer—monomer and, ultimately, intermolecular polymer—polymer attraction<sup>15–17</sup> even in the presence of favorable polymer—solvent interactions. Phase separation at the high-pressure UCST for the PDMS—CO<sub>2</sub> system appears to occur at marginal solvent conditions ( $-2 < k_D^\phi < -1$ ), albeit not as favorable conditions as the PEB<sub>10</sub>—DME<sup>6</sup> system. Also, here  $k_D^\phi$  is observed to be decreasing upon approach to this phase boundary while  $k_D^\phi$  was increasing in the PEB<sub>10</sub>—DME system.<sup>6</sup> In both cases, phase separation at the high-pressure UCST occurs for a solvent quality that is most definitely not sub-theta or poor, indicating that diminishing free volume in a high-density, compressible solvent plays a significant role in fixing the location of the phase boundary.

**Acknowledgment.** M.A.M. acknowledges the donors of the American Chemical Society Petroleum Research Fund for partial support of this research.

**Supporting Information Available:** Details on the determination of  $k_D$  from  $D$  vs  $c$  plots. This material is available free of charge via the Internet at <http://pubs.acs.org>.

## References and Notes

- (1) McHugh, M. A. In *Green Chemistry Using Liquid and Supercritical Carbon Dioxide*; DeSimone, J. M., Tumas, W., Eds.; Oxford University Press: New York, 2003; pp 125–133.
- (2) McHugh, M. A.; Krukonis, V. J. *Supercritical Fluid Extraction: Principles and Practice*, 2nd ed.; Butterworth-Heinemann: Boston, 1994.
- (3) de Gennes, P.-G. *Scaling Concepts in Polymer Physics*; Cornell University Press: Ithaca, NY, 1979.
- (4) Rubinstein, M.; Colby, R. H. *Polymer Physics*; Oxford University Press: Oxford, 2003.
- (5) Kermis, T. W.; Li, D.; Guney-Altay, O.; Park, I. H.; van Zanten, J. H.; McHugh, M. A. *Macromolecules* **2004**, *37*, 9123–9131.
- (6) Li, D.; McHugh, M. A.; van Zanten, J. H. *Macromolecules* **2005**, *38*, 2837–2843.
- (7) Gross, T.; Chen, L.; Lüdemann, H.-D. In *Supercritical Fluids as Solvents and Reaction Media*; Brunner, G., Ed.; Elsevier: Amsterdam, The Netherlands, 2004; pp 343–362.
- (8) Yamakawa, H. *Modern Theory of Polymer Solutions*; Harper and Row: New York, 1970.
- (9) Allison, S. A.; Chang, E. L.; Schurr, J. M. *Chem. Phys.* **1979**, *38*, 29–41.
- (10) Tsunashima, Y.; Hashimoto, T.; Nakano, T. *Macromolecules* **1996**, *29*, 3475–3484.
- (11) Cotts, P. M.; Selser, J. C. *Macromolecules* **1990**, *23*, 2050–2057.
- (12) André, P.; Folk, S. L.; Adam, M.; Rubenstein, M.; DeSimone, J. M. *J. Phys. Chem. A* **2004**, *108*, 9901–9907.
- (13) Xiang, Y.; Kiran, E. *Polymer* **1995**, *36*, 4817–4826.
- (14) CO<sub>2</sub> properties as a function of temperature and pressure are obtained from: Thermophysical Properties of Fluid Systems. Lemmon, E. W.; McLinden, M. O.; Friend, D. G. In *NIST Chemistry WebBook*; NIST Standard Reference Database Number 69; Linstrom, P. J., Mallard, W. G., Eds.; National Institute of Standards and Technology, Gaithersburg, MD, June 2005 (<http://webbook.nist.gov>).
- (15) Gromov, D. G.; de Pablo, J. J. *Fluid Phase Equilib.* **1998**, *150*, 657–665.
- (16) Luna-Barcenas, G.; Gromov, D. G.; Meredith, J. C.; Sanchez, I. C.; de Pablo, J. J.; Johnston, K. P. *Chem. Phys. Lett.* **1997**, *278*, 302–306.
- (17) Luna-Barcenas, G.; Meredith, J. C.; Sanchez, I. C.; Johnston, K. P.; Gromov, D. G.; de Pablo, J. J. *J. Chem. Phys.* **1997**, *107*, 10782–10792.

MA0523163